

Diffusional Characteristics of Coextruded Linear Low-Density Polyethylenes Prepared from Different Conditions of Processing

J. P. G. VILLALUENGA,¹ B. SEOANE,¹ V. COMPAÑ²

¹Departamento de Física Aplicada I, Facultad de Física, UCM, 28040 Madrid, Spain

²Departamento de Ciencias Experimentales, Universitat Jaume I, 12080 Castellón, Spain

Received 26 September 1997; accepted 27 February 1998

ABSTRACT: The permeability and diffusivity of oxygen, carbon dioxide, nitrogen, and helium have been obtained for a range of linear low density polyethylene (LLDPE) films prepared from the same raw materials but with different processing conditions. The measurements were carried out by means of a permeation technique over the temperature interval where the α -relaxation processes were observed in earlier studies. The temperature dependence of the permeability and diffusion coefficients of gases shows 2 well-differentiated regions in all films. The break temperature of these regions is approximately located at the same temperature as the α -relaxation takes place. Both the permeability and their temperature dependence do not show a noticeable influence on the processing conditions. The effect of processing conditions on the diffusivity seems to be more complex. Differences are observed for different films in the diffusion coefficients, in the case of oxygen, and in their change with the temperature, which is particularly marked in the case of carbon dioxide. Fujita's free volume model has been applied to diffusivity data in order to study the influence of films microstructure in gas permeation properties through them. © 1998 John Wiley & Sons, Inc. *J Appl Polym Sci* 70: 23–37, 1998

Key words: gas permeation; LLDPE films; diffusion

INTRODUCTION

The study of gas diffusion through membranes has been developed by different investigators to determine selectivities, apparent diffusion coefficients, and permeabilities, but the mechanism involved in the diffusional transport is poorly understood.^{1–3} The permeation rate through polymer films is governed by the size of the permeate

molecules and the dynamics of the molecular chains,^{4,5} being the last effect straightforwardly related to the structure of the chains. In this way, recent studies⁶ carried out on compression-molded films have suggested that the mobility could be decreased and the transport likely occurs in a small volume fraction of a less-dense boundary phase. This fact shows that the diffusional processes is conditioned by the free volume, and, therefore, sorption and diffusion take place almost exclusively through the amorphous regions.

Different investigators^{7–9} suggested that the gas transport in semicrystalline polyethylene films occurs nearly exclusively through the non-crystalline phase, so that the crystalline regions only act as physical barriers to impede the flow.

Correspondence to: V. Compañ.

Contract grant sponsors: DGICYT and Fundació Caixa-Castelló; contract grant numbers: PB95-0134-C02 and P1B95-04, respectively.

Journal of Applied Polymer Science, Vol. 70, 23–37 (1998)

© 1998 John Wiley & Sons, Inc.

CCC 0021-8995/98/010023-15

This fact permits to relate the fractional free volume to relative fraction of amorphous phase in the polyethylene film. The physical barriers to gas permeation provided by the crystalline entities and their influence on the packing density in the relatively ordered crystalline–amorphous interfaces will depend on the molecular orientation of the films. The microstructure of the films is governed by the chemical structure and composition of the linear low-density raw materials and processing conditions.

Preliminary studies,^{10,11} which were carried out in similar polyethylenes films, have focused on the interpretation of the spectra for the temperature intervals over which the oxygen and carbon dioxide permeation studies were performed, with the aim of comparing the changes occurring in the spectra with those observed in the permeability measurements. In other articles, the relationship between thermomechanical and diffusive effects in LLDPE films subject to longitudinal and transversal tensile drawing was investigated.¹² Finally, we also have studied the effect of annealing on the permeation characteristics of gases of LLDPE films.^{13,14}

In this article, we describe a comparative study of the temperature dependence of both permeability and diffusion coefficients in 3 different polyethylenes in terms of Fujita's free volume model, assuming that this volume is now one relative variation of the specific volume of amorphous and crystalline phases of linear low-density polyethylene (LLDPE). The effect of the composition of the LLDPE and the processing conditions on the gas permeation characteristics of films has been investigated.

EXPERIMENTAL

Characteristics of LLDPE Films

The raw materials used in the preparation of the films used in this study are 1-octene-*co*-ethylene copolymers with roughly 8% mol content of the first comonomer. The films were made up of 3 layers, that is C(15 wt %), A(70 wt %), and B (15 wt %). Layers C and A are Dowlex 2247 ($\rho = 0.917 \text{ g cm}^{-3}$), and the third layer (B) is Dowlex 2291 ($\rho = 0.912 \text{ g cm}^{-3}$). The thickness of the first, second, and third layers were 3.5, 16, and 3.5 μm , respectively. The 3 films used, which will be called LLDPE 1, LLDPE 12, and LLDPE 14, were obtained by coextrusion using the same raw ma-

terials but with different processing conditions. Thus, the distances between die and chill roll were 15, 10, and 5 mm, respectively, for LLDPE 1, LLDPE 14, and LLDPE 12. Another difference in the processing conditions was that the vacuum knife depression for LLDPE 1, LLDPE 14, and LLDPE 12 films amounted to 2, 3, and 5 cm Hg, respectively. The speed of the three extruders C, A, and B, which were 88, 29, and 88, respectively, and the die-exit temperature kept at 543 K, were the same for all the LLDPE films. Finally, it should be mentioned that the line speed was 200 rpm in all cases.

The thermal behavior of the films was determined with a DSC-821 Mettler Toledo calorimeter at a heating rate of 10°C/min. The thermogram of the films shows a small melting peak in the vicinity of 40°C in all films. These peaks correspond, presumably, to the fusion of very small crystalline entities, followed by a wide melting endotherm that extends from 90 up to 125°C, with the maximum of the peak centered at 120°C. The degree of crystallinity of the films, determined from the melting endotherms by assuming that the melting enthalpy is $960 \text{ cal (mol CH}_2\text{)}^{-1}$, was found to be 0.25, 0.24, and 0.30, respectively, for LLDPE 1, LLDPE 14, and LLDPE 12.

The crystallinity of the films was also determined by Raman spectroscopy using a Ramanor U 1000 double monochromator equipped with 2 1800 g mm^{-1} planar holographic gratings. The spectra present 2 peaks in the 3 films centered at 1418 and 1077 cm^{-1} , which are considered to be associated, respectively, with the crystalline and amorphous phases.¹⁵ By comparing the intensities of these peaks with that of the peak located at 1296 (independent of the morphology of the films), one finds that the crystallinity–amorphous fractions of the LLDPE 1, LLDPE 14, and LLDPE 12 films are 0.25/0.62, 0.24/0.60, and 0.30/0.57, respectively. According, the fraction interfacial material for LLDPE 1, LLDPE 14, and LLDPE 12 amounts to 0.13, 0.16, and 0.13, respectively.

The films exhibit birefringence as a consequence of their orientation in the direction of extrusion. The value Δn , measured with an Amplival Pal microscope at room temperature, was $1.4 \cdot 10^{-3}$, $2.9 \cdot 10^{-3}$, and $2.6 \cdot 10^{-3}$ for LLDPE 1, LLDPE 14, and LLDPE 12, respectively.

Permeability Measurements

The permeability measurements of gases through the films were carried out by using an experimen-

tal setup that has been described elsewhere.^{10–14} The permeation of the oxygen and carbon dioxide was measured through LLDPE 1 and LLDPE 12, and oxygen, carbon dioxide, nitrogen, and helium through LLDPE 12. Values of the transport coefficients of the pure gases through the 3 above-mentioned films were determined in the temperature interval of 298–358 K by a standard device in which 2 chambers coupled to pressure sensors are separated by the membrane whose permeation is to be measured. Measurements of the rate of increase in the pressure of the gas at the downstream pressure chamber, p_1 , and the value of the upstream pressure, p_0 , were obtained by means of Leybold-CM3 pressure transducers with full-scale ranges of 10 mm Hg and 10^3 mm Hg, respectively, and monitored by computer. The experimental device was immersed in a thermostat bath Techne TU-16D, whose temperature was measured and controlled with PT100 sensors with accuracy of $\pm 0.1^\circ\text{C}$. The area of the films, which was assumed to be the same as that of O-ring opening, which is in direct contact with the sample, was 5 cm^2 . The volume in the downstream reservoir was measured by using the helium expansion technique. The value of this volume was fixed at 9.0 cm^3 by convenience in order to get downstream pressures sufficiently low in comparison with the pressure in the upstream side. In all experiments, the relation $p_1 < 0.01 p_0$ was satisfied.

RESULTS AND DISCUSSION

The transport of gases through membranes is generally expressed in terms of the apparent permeability P and the apparent diffusion coefficient D . The permeability coefficient, under conditions of steady-state permeation, can be evaluated by means of the following expression¹⁰:

$$P_{\text{app}} = \frac{273}{76} \cdot \frac{V \cdot L}{A \cdot T \cdot p_0} \cdot \frac{dp(t)}{dt} \quad (1)$$

where V is the volume of the low-pressure chamber, A is the effective area of the film, L is the thickness of the membrane, p_0 is the pressure in cm of Hg of the penetrant gas in the upstream chamber, T is the absolute temperature of the measurement, and $dp(t)/dt$ is the rate of pressure measured by the pressure sensor in the low-pressure chamber.

The diffusion coefficient was obtained from the intercept with the time axis θ of the plot p_1 against t , as suggested by Barrer¹⁶

$$D_{\text{app}} = \frac{L^2}{6\theta} \quad (2)$$

Values of the P and D were quite well reproducible, with standard deviations being ± 2 and $\pm 20\%$, respectively. Once P and D are calculated, the apparent solubility coefficient S may be evaluated by means of the following expression in convenient units:

$$S_{\text{app}} = \frac{P}{D} \quad (3)$$

Owing to the relatively low values of θ obtained for the very thin LLDPE films used in this study ($\cong 25\mu\text{m}$), significant errors could be obtained in the determination of the diffusion coefficient by this method. Actually, the smaller the thickness, the lower θ and, consequently, the larger the uncertainty of the value of D obtained. In order to increase the magnitude of the time lag and thus reducing the uncertainty of the D values, transport measurements were performed in LLDPE films made up of 4 films firmly stacked with a rolling cylinder at room temperature, similar to

Table I Illustrative Example of the Time Lag Values Estimated for N_2 Gas in Different Films of LLDPE 12 Firmly Stacked for the Whole Range of Temperature Studied

Temperature ($^\circ\text{C}$)	Time Lag (s)			
	2 Films	4 Films	8 Films	12 Films
25	15.2	52.7	112	298
30	11.0	38.7	90.9	245
35	9.2	29.6	69.1	183
40	7.5	21.9	54.3	144
45	6.1	16.4	42.9	111
50	5.0	13.3	34.8	90.0
55	4.1	10.4	28.7	72.0
60	3.6	8.5	23.9	61.2
65	2.8	7.4	21.0	53.2
70	2.3	6.0	18.0	45.3
75	1.9	5.4	15.6	36.0
80	1.5	4.3	13.8	31.4
85	1.3	3.7	12.2	26.6

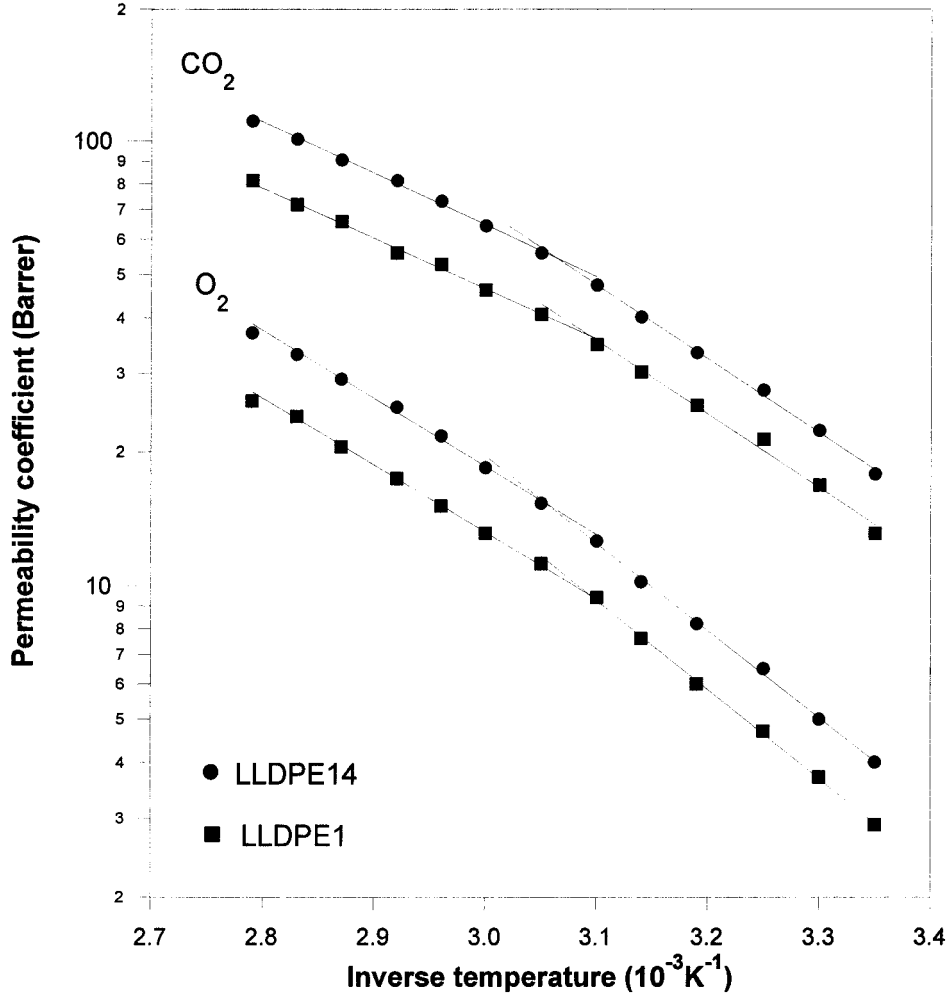


Figure 1 Arrhenius plots for the permeability coefficient of oxygen and carbon dioxide through LLDPE 1 and LLDPE 14.

the study carried out on the effect of the annealing in coextruded LLDPE films where boundary effects at the interface between films were not detected.^{13,14}

Earlier studies carried out on the diffusion gases through multilayer membranes showed that the relation between the time lag of the whole multilayer system and that of a single layer is given by¹⁷

$$\theta = \left[\sum_{i=1}^n \left\{ \frac{l_i^{i-1}}{D_i} \prod_{j=0}^{i-1} k_j \right\} \right]^{-1} \times \left[\sum_{i=1}^n \left\{ \frac{l_i^2}{2D_i} \sum_{i=1}^n \left[\frac{l_i^{i-1}}{D_i} \prod_{j=0}^{i-1} k_j \right] - \frac{l_i^3}{3D_i^2} \prod_{j=0}^{i-1} k_j \right\} \right]$$

$$+ \sum_{i=1}^n \left\{ \frac{l_i^{i-1}}{D_i} \left(\prod_{j=0}^{i-1} k_j \right) \sum_{\beta=i+1}^n \left[\frac{l_\beta}{\prod_{j=0}^{\beta-1} k_j} \sum_{\beta=1}^n \left[\frac{l_\beta^{\beta-1}}{D_\beta} \prod_{j=0}^{\beta-1} k_j \right] - \frac{l_\beta^2}{2D_\beta} \right] \right\} \quad (4)$$

where D_i is the diffusion coefficient of the diffusant in the i th component phase, where $i = 1, 2, \dots, n$, and is assumed to be independent of concentration, time, or positional coordinate; k_i is the distribution coefficient between the 2 fazes; and l_i is the thickness of the each slab. In our case

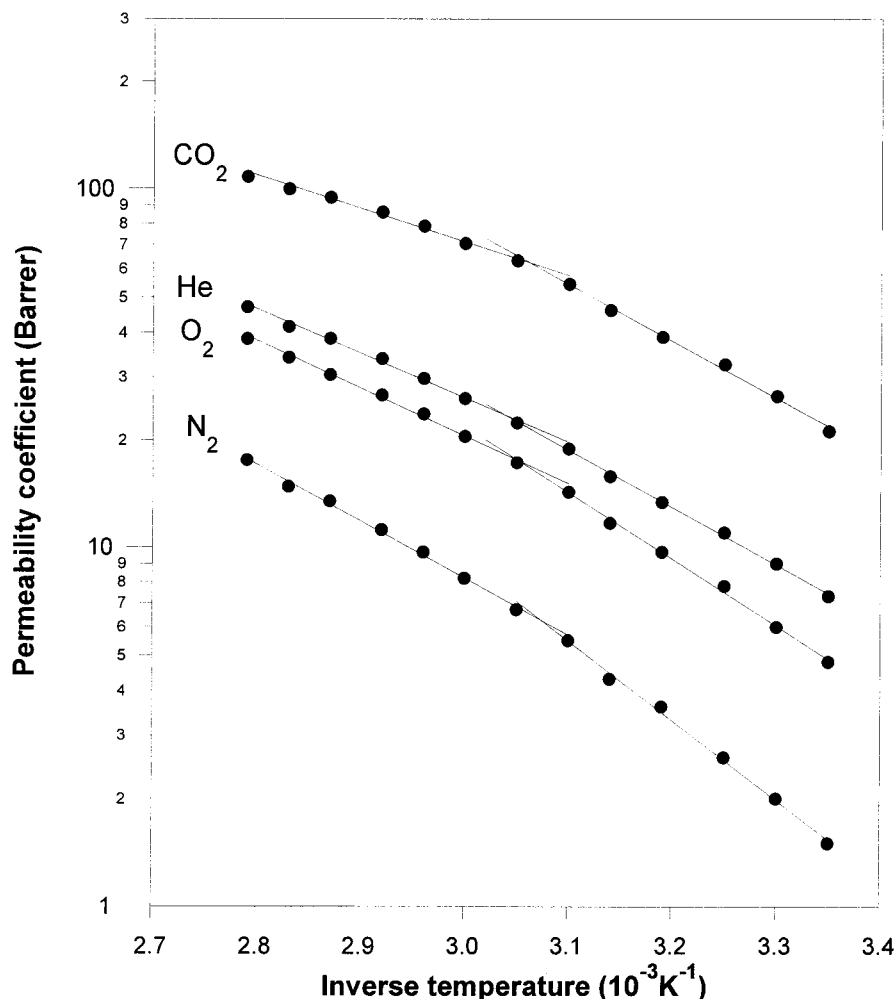


Figure 2 Arrhenius plots for the permeability coefficient of oxygen, carbon dioxide, nitrogen, and helium through LLDPE 12.

($n = 4$), the time lag, taking $k_i = 1$, D_i and l_i identicals in each layer, will be

$$\theta = 10 \cdot \theta_1 + f(l_i, D_i, k_i) \quad (5)$$

where $f(l_i, D_i, k_i) = 6\theta_1$ when we are in the ideal case.

The experimental values obtained for the time lags in different multilayers of LLDPE 12 films for whole range of temperatures studied are given as an example in Table I. In this table, it can be observed that if the number of the stacked films increase, the time lag increases; consequently, the uncertainty in the evaluation of the diffusion coefficient decreases. It should be mentioned that the stacking of LLDPE films is apt to result in systematic errors in the determination of P and D coefficients. These errors have been estimated,

and some attempts have been made in order to reduce them, as can be seen in recent publications.¹⁴ Following Shishatskii and coworkers,¹⁸ the configuration of the gas permeation apparatus and the permeation experiments were conceived in such a manner that systematic errors introduced by the stacking of the films were noticeably reduced. It has been reported that the permeability coefficients of gases obtained in stacked samples did not seem to be affected by the stacking. However, significant variations were found in the diffusion coefficients measured in stacked LLDPE films. This result was analyzed and interpreted according to current theories. All these circumstances were taken into account in the present work, so the results are carefully checked, and all the erratic runs were eliminated from further consideration.

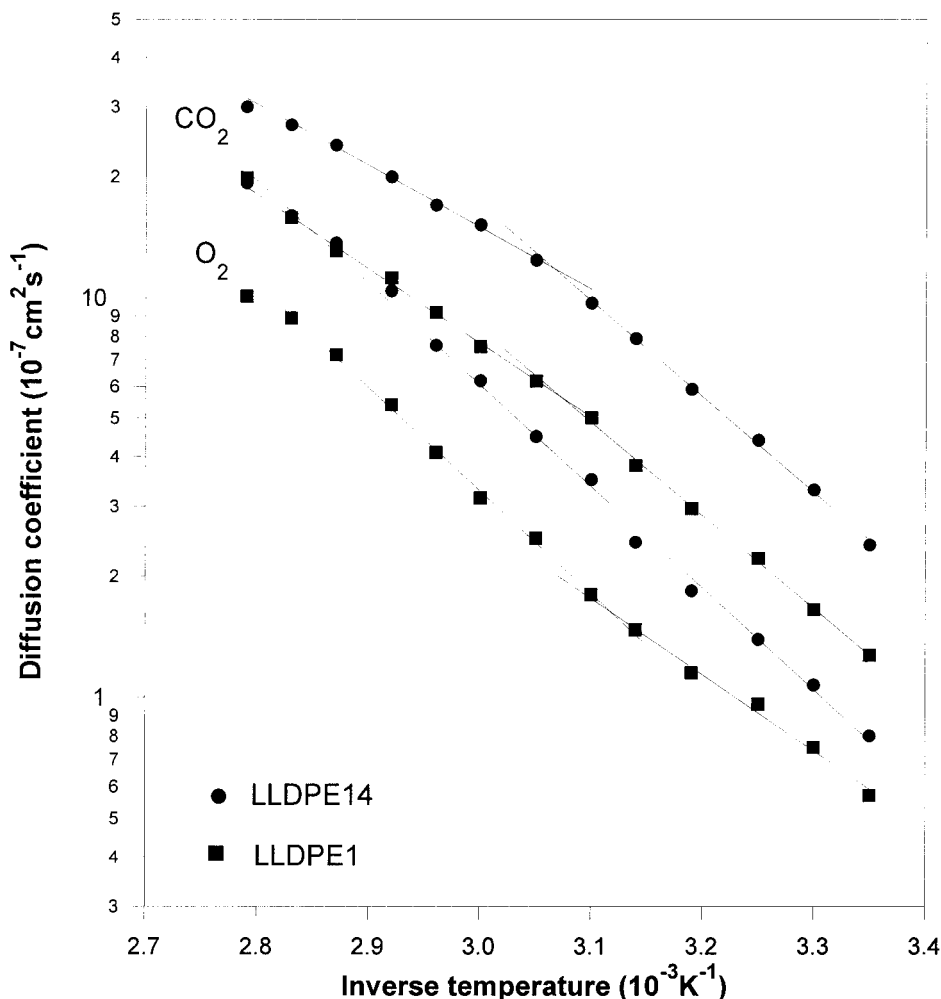


Figure 3 Arrhenius plots for the diffusion coefficient of oxygen and carbon dioxide through LLDPE 1 and LLDPE 14.

The temperature dependence of permeability coefficient of O₂ and CO₂ through the LLDPE 1 and LLDPE 14 films and N₂, O₂, He, and CO₂ through the LLDPE 12 films are shown in Figures 1 and 2. The permeability coefficient of CO₂ is larger than that O₂ in LLDPE 1 and LLDPE 14 films; whereas in LLDPE 12 film, the permeability of the gases increases in the following order $P(\text{CO}_2) > P(\text{He}) > P(\text{O}_2) > P(\text{N}_2)$. Similar trends have been observed for other polyethylene films in recent investigations.¹⁹ If we compare the gas permeation between the different films, some differences between the values of gas permeability measured for a given temperature could be observed. For example, the value of P for O₂ at 25°C in the LLDPE 1 film is 2.9 barrers, whereas this value rises to 4 and 4.8 barrers in the LLDPE 14 and LLDPE 12 films, respectively.

The apparent diffusion coefficients of the gases obtained at different temperatures for LLDPE films are plotted in Figures 3 and 4. For clear comparison, the values obtained for D in LLDPE 1 and LLDPE 14 are shown in the same figure. A similar behavior as in the permeability results for LLDPE 1 and LLDPE 14 can be observed, since the D for CO₂ is larger than D for O₂. In the case of LLDPE 12 film, the D values for He are significantly larger than the D values for the rest of the gases, whose values are nearly the same. In contrast to permeability values, the diffusivity of the gases increases in the following order: $D(\text{He}) > D(\text{O}_2) > D(\text{CO}_2) \cong D(\text{N}_2)$. The results also indicate that the gas diffusion seems to be higher in LLDPE 12 than in LLDPE 1 and LLDPE 14, as it has been observed in permeability. For example, the value of D for O₂ at 25°C in the LLDPE 1 film

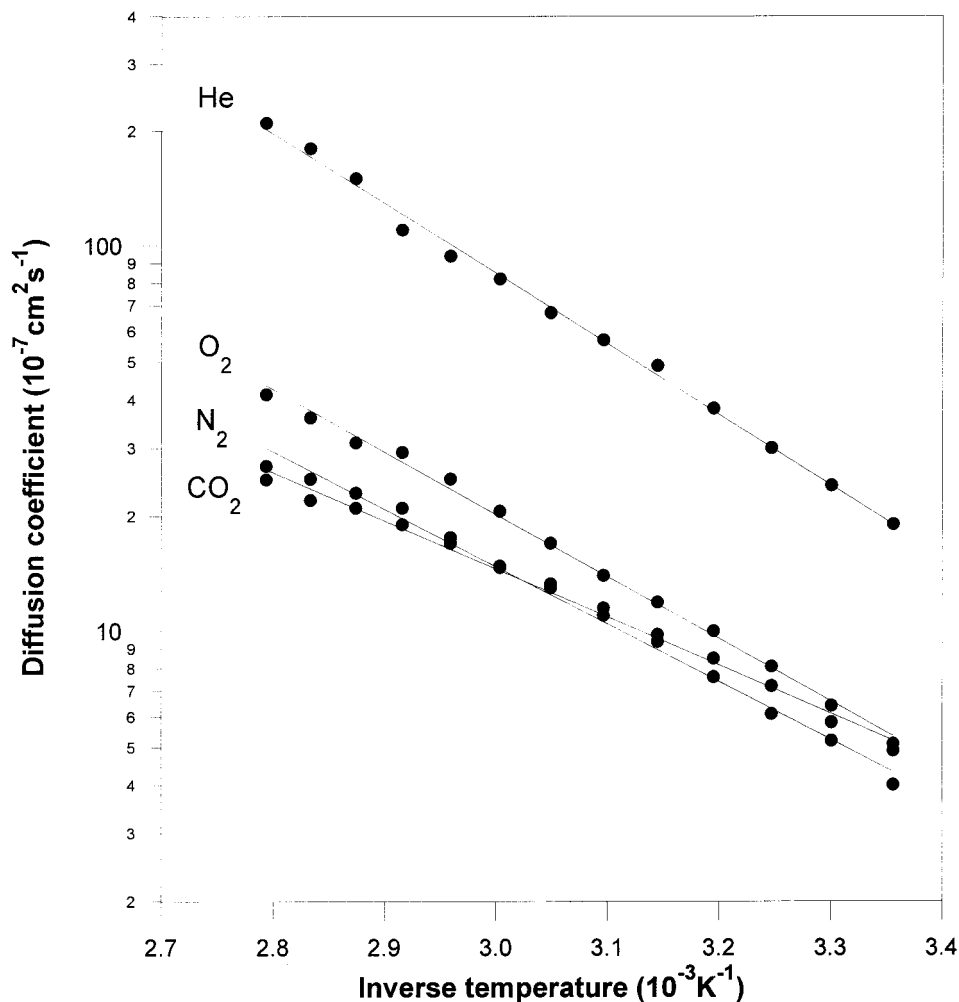


Figure 4 Arrhenius plots for the diffusion coefficient of oxygen, carbon dioxide, nitrogen, and helium through LLDPE 1.

is $4.7 \times 10^{-8} \text{ cm}^2 \text{ s}^{-1}$ and $8.0 \times 10^{-8} \text{ cm}^2 \text{ s}^{-1}$ in the LLDPE 14 film, and it reaches to $5.1 \times 10^{-7} \text{ cm}^2 \text{ s}^{-1}$ in LLDPE 12.

The change of behavior between permeability and diffusion coefficients found in LLDPE 12 suggests that the solubility of the permeate gas may play an important role in the permeation process through LLDPE films. The effect of the solubility could be due to the fact that the small crystals formed in the amorphous zone have less volume; consequently, the gas solubility in the polymer increases and so does the permeability. These changes in the diffusion and in the permeability are much greater in the high-temperature region. This fact might be due to the melting of small and less perfect crystalline entities. This melting process might increase the solubility of the gases in the films, on the one hand, and favor the ease of

the gas diffusion due to the decrease of the obstruction of the diffusion paths, on the other hand, so that the permeability through the films increases.

The study of gas permeation in LLDPE films reveals that there is not any correlation between the permeability coefficient and the physical characteristics of the diffusing molecule; however, it is clear from Figure 5 that the diffusion coefficient decreases as the size of the diffusing molecule increases. In contrast, as is shown in Figure 6, the solubility coefficient increases with increasing molecular dimensions. These tendencies are in accordance with the general trend observed in other polymers.²⁰

On the assumption that the films are homogeneous systems, the transport of gases through the films may be described as a thermally activated

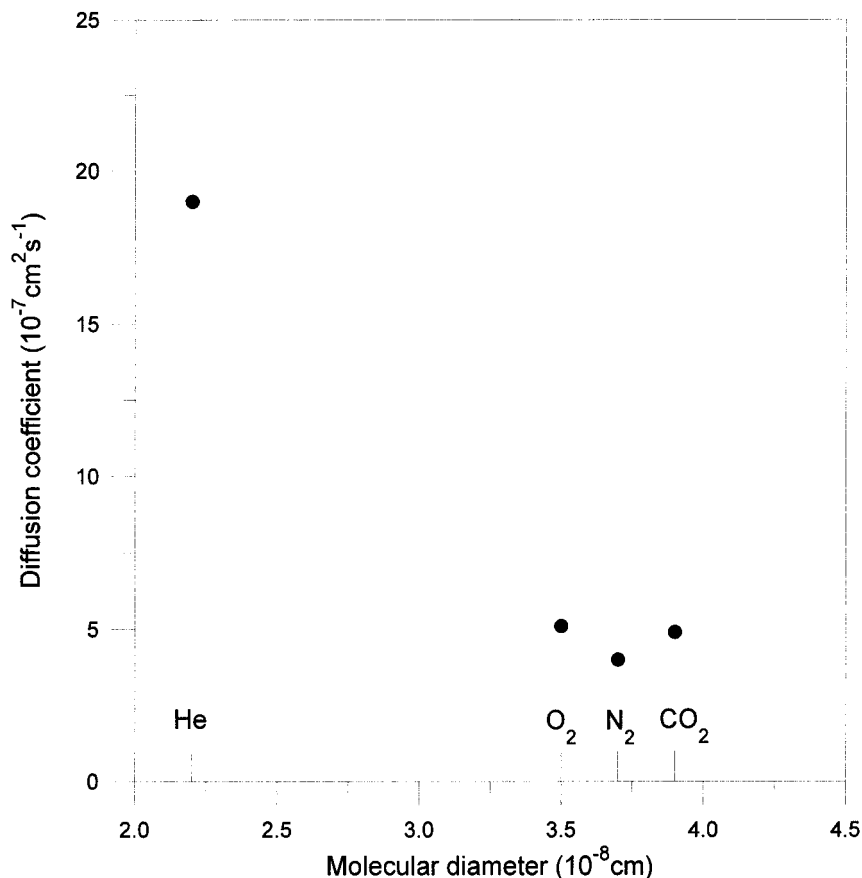


Figure 5 Diffusion coefficient versus molecular diameter of gases for LLDPE 12 films at 25°C.

process that obey the Arrhenius equation given by

$$X = X_0 \exp\left(-\frac{E_x}{RT}\right) \quad (6)$$

where X represents the permeability or diffusion coefficient, P and D , E_x becomes the activation energy of the permeability E_p or the activation energy of diffusion E_D , and X_0 is a constant (P_0 or D_0), which is characteristic of the polymer-permeate system. Consequently, activation energies associated with these processes may be determined from the semilogarithmic plots shown in Figures 1 to 4.

A close inspection of these figures suggests the following 2 different behavior: one covering the temperature interval 298–323 K, and another from 328 to 358 K, for LLDPE 1 and LLDPE 12. We can observe similar variations for LLDPE 14, but the intervals are slightly shifted to 298–328

and 333–358 K. The fitting of the permeability values to straight lines is satisfactory in all cases. The activation energies are presented in Table II. A significant decrease in the activation energy of the permeability can be detected in going from the low-temperature to high-temperature interval, presumably as a consequence of the increase in solubility arising from initiation of the melting of the smaller crystalline entities. The activation energy for the permeability in the 298–323 K interval is somewhat lower than that previously reported for oriented PE,²¹ presumably as a consequence of the low crystallinity of the coextruded LLDPE films studied in this article. Similar Arrhenius plots over the temperature intervals indicated above also give a good representation of the temperature dependence of the gas diffusion coefficient. The values obtained for activation energy from the plots are also given in Table II. We can observe in Table II that the films LLDPE 1 and LLDPE 14 follow, for activation energy,

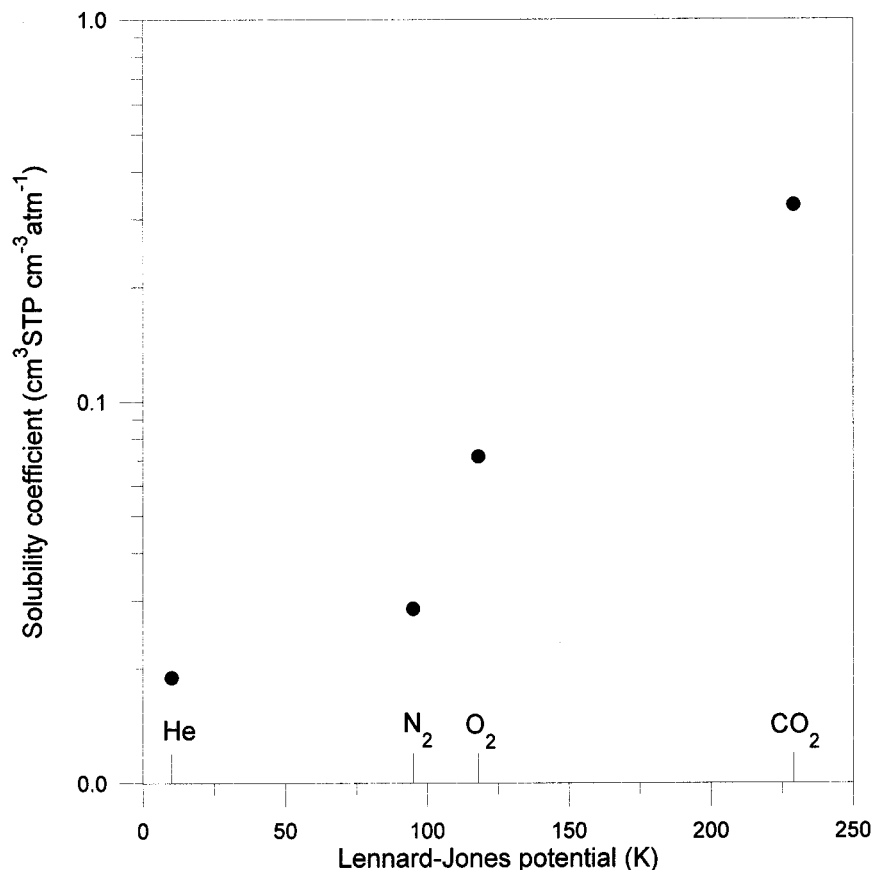


Figure 6 Solubility coefficient of gases in function of Lennard–Jones potential for LLDPE 12 films at 25°C.

the trend $E_D(\text{O}_2) > E_D(\text{CO}_2)$ and $E_P(\text{O}_2) > E_P(\text{CO}_2)$. In LLDPE 12, the trend is $E_D(\text{CO}_2) > E_D(\text{O}_2) > E_D(\text{N}_2) > E_D(\text{He})$ and $E_P(\text{N}_2) > E_P(\text{O}_2) > E_P(\text{He}) > E_P(\text{CO}_2)$. Consequently, the heat of solution $\Delta H = E_P - E_D$ decreases from oxygen to carbon dioxide in LLDPE 1 and LLDPE 14 and decreases from nitrogen to carbon dioxide in

LLDPE 12. The values of ΔH for the films and each gas studied are also given in Table II. It is worth noting that the values for diffusion activation energy are higher than that obtained for permeability activation energy in LLDPE 1 and LLDPE 14. The activation energy of the permeability is relatively higher in the LLDPE 12 for all

Table II Activation Energy in kJ/mol for the Oxygen, Carbon Dioxide, Nitrogen, and Helium Obtained from Permeabilities and Diffusion Coefficient Measurements Through LLDPE 1, LLDPE 12, and LLDPE 14

Film	Temperature Interval (°C)	E_P Permeability				E_D Diffusion			
		CO ₂	O ₂	N ₂	He	CO ₂	O ₂	N ₂	He
LLDPE 1	25–50	31.7	38.4	—	—	47.1	45.6	—	—
LLDPE 1	50–85	21.9	27.8	—	—	36.8	44.2	—	—
LLDPE 12	25–50	—	35.3	39.7	30.2	—	33.5	31.7	27.4
LLDPE 12	50–85	—	24.9	28.6	27.4	—	25.5	22.5	25.8
LLDPE 14	25–50	31.8	37.6	—	—	43.8	46.8	—	—
LLDPE 14	50–85	21.8	28.3	—	—	32.8	47.1	—	—

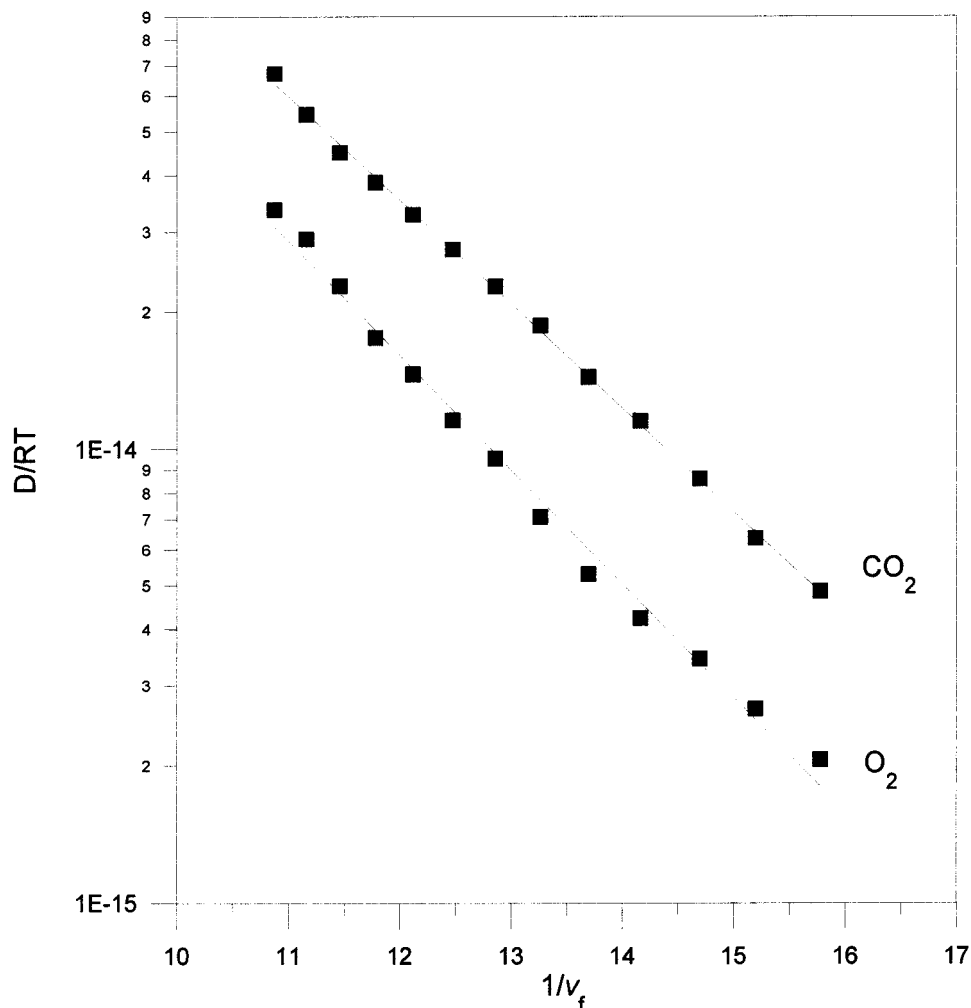


Figure 7 Dependence of the diffusion coefficient on the free volume for oxygen and carbon dioxide in LLDPE 1 films.

gases than the activation energy of the diffusion. This behavior suggests that gas diffusion through the films may not be a single activated processes as a consequence of the morphological changes caused by recrystallization processes. The fact that the activation energy values for diffusion in LLDPE 12 are lower than that LLDPE 1 and LLDPE 14 suggests that the obstruction to the diffusion process produced by the crystalline microstructure is somewhat lower in the first film, as was revealed by other investigators.^{22,23}

The effects of the polymer on the diffusivity were taken into account by Michaels and Parker²² and Michaels et al.²³ who expressed the diffusion coefficient by means of

$$D = \frac{D^*}{\tau\beta} \quad (7)$$

where D^* is the apparent diffusion coefficient for completely amorphous polymers and, consequently, only depends on the nature of the diffusant. The parameter τ reflects the tortuosity of the path caused by the presence of crystalline entities, whereas β is mainly related with the lack of mobility in the amorphous regions close to the anchoring points in the crystals.²² The comparison of the values of diffusion coefficients in LLDPE films permits to relate qualitatively the differences observed in the D values to differences in the structural parameter mentioned above and to put into relation the diffusion coefficients and the crystalline and amorphous fractions in the films. In this way, when we compare the values obtained for the apparent diffusion coefficients in the 3 films, the values in the LLDPE 12 are significantly larger than the values in the other

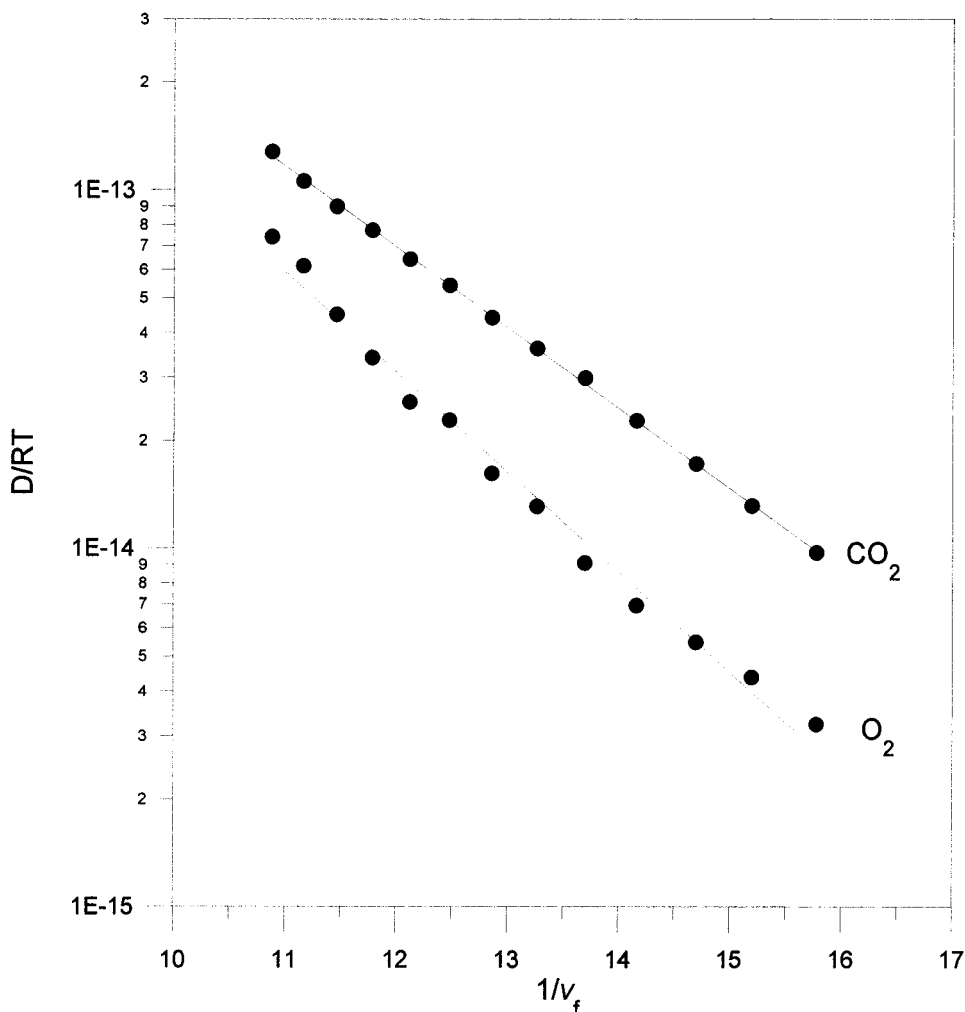


Figure 8 Dependence of the diffusion coefficient on the free volume for oxygen and carbon dioxide in LLDPE 14 films.

films since the crystallinity in the first film is the largest.

The diffusion of small molecules through semi-crystalline polymers can be expressed in terms of Fujita's free volume model²⁴ by means of the following expression:

$$D = RTA_d \exp\left(\frac{B_d}{\phi_a v_f}\right) \quad (8)$$

where ϕ_a is the volume fraction of amorphous polymer, v_f is the fractional free volume, R is the universal gas constant, T is the absolute temperature, and A_d and B_d are characteristic parameters of the system. The last parameters are dependent on the size and shape of the penetrant molecule, and they are taken as independent of

temperature and penetrant concentration. The fractional free volume, which depends on the hydrostatic pressure applied on the high-pressure chamber, temperature, and the penetrant concentration expressed as a free volume v , can be written as

$$v_f = v_{fs}(T_s, p_s, 0) + \alpha(T - T_s) - \beta(p - p_s) + \gamma v \quad (9)$$

where $v_{fs}(T_s, p_s, 0)$ is the fraction free volume of the polymer at some reference temperature T_s and pressure p_s , $\alpha = (\partial v_f / \partial T)_S$ is the thermal expansion coefficient, $\beta = (\partial v_f / \partial p)_S$ is the compressibility coefficient, and $\gamma = (\partial v_f / \partial v)_S$ is a coefficient that defines the effectiveness of the penetrant as a plasticizer. At low pressure, like those used in this work, following Stern and coworkers,²⁵ the

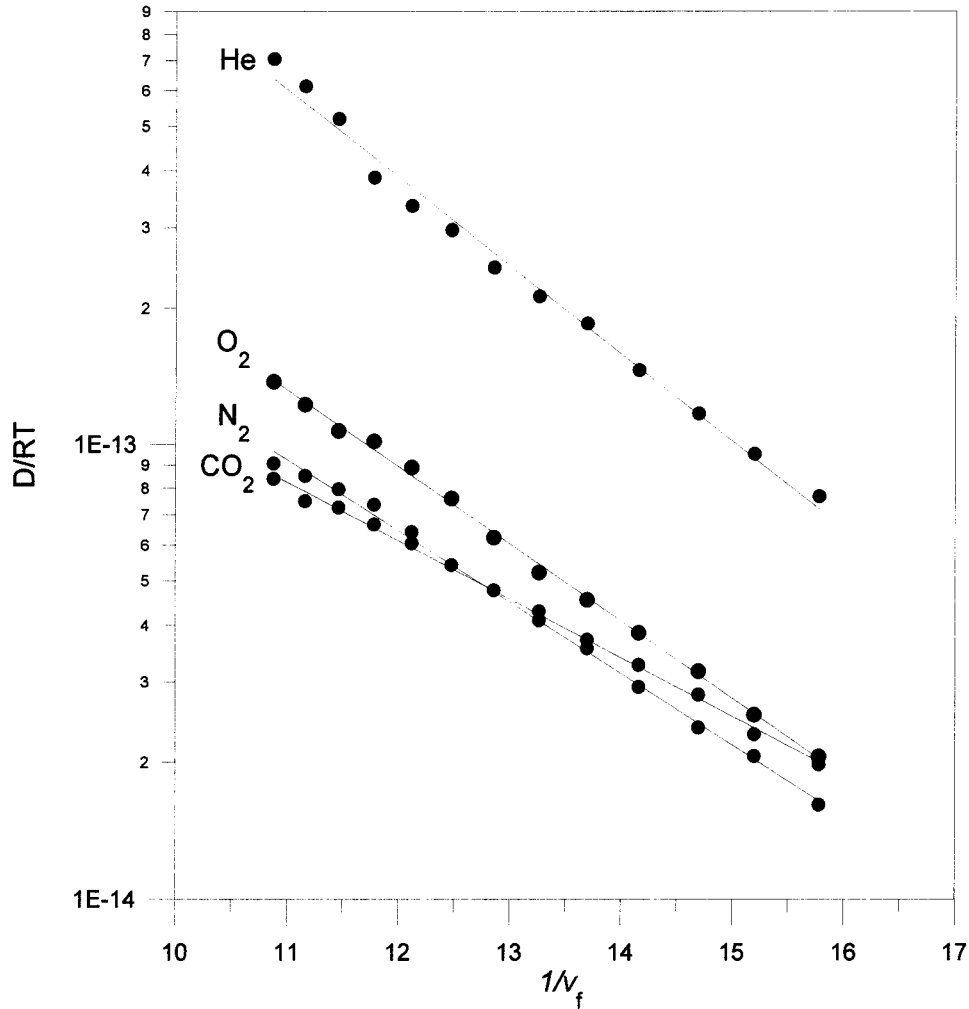


Figure 9 Dependence of the diffusion coefficient on the free volume for oxygen, carbon dioxide, nitrogen, and helium in LLDPE 12 films.

fractional free volume expression given by eq. (8) can be simplified as follows:

$$\nu_f = \nu_{fs}(T_s) + \alpha(T - T_s) \quad (10)$$

In this work, values of the fractional free volume as a function of temperature were obtained from the following relationship, which is a rather good approximation, as has been shown in another study¹⁴:

$$\nu_f(T) = \frac{\nu_a(T) - \nu_c(T)}{\nu_a(T)} \quad (11)$$

where ν_c and ν_a represent, respectively, the specific volume of LLDPE in crystalline and amorphous phases. Following Chiang and Flory,²⁶ the

temperature dependence of the specific volumes was made from the following relationships:

$$\nu_a(T) = 1,152 + 8,8 \cdot 10^{-4}(T - 273,15) \quad (12)$$

$$\nu_c(T) = 0,993 + 3,0 \cdot 10^{-4}(T - 273,15) \quad (13)$$

If eq. (8) is expressed in a logarithmic form,

$$\ln\left(\frac{D}{RT}\right) = \ln A_d + \frac{B_d}{\phi_a \nu_f} \quad (14)$$

it is clear that the parameters A_d and B_d may be obtained from the least squares fitting of the corresponding diffusion data in the plots of $\ln(D/RT)$ against $1/\nu_f$. As can be seen in Figures 7 to 9, the

Table III Values of the Free Volume Parameter A_d and B_d Evaluated from the Diffusion Coefficient Results Using Equation (11)

Permeant Gas	LLDPE 1	$(\phi_a = 0.65)$	LLDPE 12	$(\phi_a = 0.57)$	LLDPE 14	$(\phi_a = 0.60)$
	$A_d \cdot 10^{11}$	B_d	$A_d \cdot 10^{11}$	B_d	$A_d \cdot 10^{11}$	B_d
CO ₂	2.0	0.34	0.21	0.17	3.4	0.31
O ₂	2.3	0.39	0.97	0.22	6.1	0.38
N ₂	—	—	0.49	0.21	—	—
He	—	—	8.0	0.25	—	—

The units of A_d are $\text{m}^2 \text{gmol}^{-1} \text{J}^{-1}$, while B_d is dimensionless.

data fit fairly well to straight lines for all LLDPE films studied. The values of parameters A_d and B_d obtained for the different gases are listed in Table III.

It can be seen that the values for the A_d parameter decrease in the following order: $\text{CO}_2 < \text{O}_2$ in LLDPE 1 and LLDPE 14, and $\text{CO}_2 < \text{N}_2 < \text{O}_2 < \text{He}$ in LLDPE 12. It is also observed that these values are quite different in the 3 LLDPE films. Moreover, the values of parameter B_d , which shows the same dependence on the films as found for the parameter A_d , are significantly larger in LLDPE 1 and LLDPE 14 than the values obtained in the LLDPE 12. In the 2 first polymers, their values are very similar. These results suggest that the free volume parameters are very sensitive to the structural characteristics of the films in the sense that both A_d and B_d are larger for the films, which exhibit high birefringence. It should be pointed out that the values thus obtained for A_d involve some uncertainty owing to the fact that it is necessary to extrapolate to $1/\nu_f = 0$ from rather limited values of ν_f . Stern and

coworkers²⁷ performed a thorough study on the permeation of gases through polyethylene films, finding that the values of A_d and B_d for CO_2 are $5.4 \times 10^{-11} (\text{m}^2 \text{gmol}^{-1} \text{J}^{-1})$ and 0.40, respectively. Whereas in these results, the value of B_d compares satisfactorily with that given for CO_2 in LLDPE films, and the value of A_d is somewhat higher than found in these films.

The permselectivity of LLDPE films expressed in terms of permeability ratios is given in Tables IV and V. The values obtained for LLDPE 14 are quite similar to LLDPE 1. A close inspection of these tables reveals that the permselectivity decreases as the temperature increases. For example, the decrease in selectivity varies from 10% for $\text{P}(\text{CO}_2)/\text{P}(\text{He})$ to 50% for $\text{P}(\text{CO}_2)/\text{P}(\text{N}_2)$ in LLDPE 1 film. In the case of LLDPE 12 and LLDPE 14 films, this decrease is approximately the same so that it amounts to 17% for $\text{P}(\text{CO}_2)/\text{P}(\text{He})$ and 49% for $\text{P}(\text{CO}_2)/\text{P}(\text{N}_2)$. We think that the decrease in permselectivity with the temperature is a consequence of the decrease in diffusivity or mobility selectivity (we can observe this when we compare

Table IV Permselectivity of LLDPE 1 Film Expressed in Terms of Permeability Ratios

T (°C)	CO_2/He	CO_2/O_2	CO_2/N_2	He/O_2	He/N_2	O_2/N_2
25	2,9	4,4	13	1,5	4,4	2,9
30	3,0	4,4	13	1,5	4,2	2,9
35	2,9	4,1	12	1,4	4,1	2,9
40	2,8	4,0	11	1,4	3,8	2,7
45	2,8	4,0	10	1,3	3,6	2,6
50	2,8	3,7	9,9	1,3	3,5	2,7
55	2,7	3,6	9,0	1,3	3,3	2,5
60	2,7	3,6	8,6	1,3	3,2	2,4
65	2,7	3,4	8,0	1,3	3,0	2,4
70	2,6	3,2	7,5	1,2	2,9	2,3
75	2,4	3,0	6,8	1,2	2,8	2,3
80	2,3	2,9	6,7	1,3	2,8	2,2
85	2,3	2,9	6,5	1,2	2,7	2,3

Table V Permselectivity of LLDPE 12 Film Expressed in Terms of Permeability Ratios

T (°C)	CO_2/He	CO_2/O_2	CO_2/N_2	He/O_2	He/N_2	O_2/N_2
25	2,9	4,4	13	1,5	4,6	3,0
30	2,9	4,4	13	1,5	4,6	2,9
35	2,9	4,2	12	1,4	4,3	3,0
40	2,9	4,0	11	1,4	3,8	2,7
45	2,9	3,9	11	1,4	3,7	2,7
50	2,9	3,8	9,9	1,3	3,5	2,6
55	2,8	3,7	9,7	1,3	3,5	2,7
60	2,7	3,4	8,6	1,3	3,2	2,5
65	2,7	3,3	8,2	1,2	3,1	2,5
70	2,6	3,2	7,8	1,2	3,0	2,4
75	2,5	3,1	7,4	1,2	3,0	2,4
80	2,4	3,0	7,1	1,2	2,9	2,4
85	2,4	2,8	6,6	1,2	2,7	2,3

the values of $D(\text{O}_2)/D(\text{N}_2)$ for each temperature), as has been obtained by Koros.²⁸

CONCLUSIONS

The results discussed above suggest that the gas permeation through LLDPE films is a rather complex process in which the permeation in these samples does not show a noticeable influence on the processing conditions since only small variations in permeability and diffusion coefficients and their temperature dependence, among 3 different samples, are detected. This fact, together with the results reported in preliminary studies, in which both the variation of the gas applied pressure and the tensile drawing of the samples had a little effect on the gas permeation characteristics of the samples, makes LLDPE films suitable for the use in the packaging industry.

The analysis of the temperature dependence of the permeability and diffusion coefficients of gases through these films showed, in all cases, a significant increase in the values of P and D with the temperature in 2 different intervals. The break temperature of these intervals correspond to α -relaxation observed in earlier studies.^{10–12} The location of these breaks with α -relaxation could be due to orientation of the coextruded films analyzed as a consequence of the fact that it arises from motions in which crystalline entities intervene.

On the other hand, the presence of octene increases the gas permeability in LLDPE films, and, therefore, a reduction in the activation energy is observed. As the diffusion coefficients and

the energy related to the diffusion process are almost the same as that found in conventional polyethylene, this behavior is associated with a change in the gas solubility as a consequence of the fusion of small crystalline entities.

Finally, we have observed that the Fujita's free volume model expressed by means of eq. (8) seems to be valid to put into relation the diffusion values with the volume fraction of free volume, which has been taken into account by eq. (11) in LLDPE samples. It is observed an increase in diffusional parameters as the fraction of interfacial material increases; probably, as a consequence of this fact, the permeability of LLDPE 14 is larger than in the other LLDPE films. This is possible according to the favoring of microcavities in the interfaces that increase the solubility.

REFERENCES

1. S. A. Stern and H. L. Frich, *Ann. Rev. Mater. Sci.*, **11**, 523 (1981).
2. J. Sonneburg, J. Gao, and J. H. Weiner, *Macromolecules*, **23**, 4653 (1990).
3. G. F. Sykes and A. K. St. Clair, *J. Appl. Polym. Sci.*, **32**, 37254 (1986).
4. K. Tanaka, H. Kita, K. Okamoto, A. Nakamura, and Y. Kusuki, *Polym. J.*, **22**, 381 (1990).
5. K. Tanaka, H. Kita, M. Okano, and K. Okamoto, *Polymer*, **33**, 385 (1992).
6. *Quality Enhancement and Process Availability in LLDPE Stretch Film by Multisensor and Computerized System*, C. Forni, Coord., Brite-Euram-BE-Project 4104, 1995.
7. A. S. Michaels and H. J. Bixler, *J. Polym. Sci.*, **50**, 393 (1961).

8. A. S. Michaels and R. B. Parker Jr., *J. Polym. Sci.*, **41**, 33 (1959).
9. A. W. Myers, C. E. Rogers, V. Stannet, and M. Szwarc, *Tappi J.*, **41**, 716 (1958).
10. V. Compañ, A. Ribes, R. Diaz-Caleja, and E. Riande, *Polymer*, **36**, 323 (1995).
11. V. Compañ, A. Ribes, R. Diaz-Caleja, and E. Riande, *Polymer*, **37**, 2243 (1996).
12. J. P. Garcia-Villaluenga, B. Seoane, V. Compañ, and R. Diaz-Calleja, *Polymer*, **38**, 3827 (1997).
13. V. Compañ, A. Andrio, Ma. L. López, and E. Riande, *Polymer*, **37**, 5831 (1996).
14. V. Compañ, A. Andrio, Ma. L. López, C. Alvarez, and E. Riande, *Macromolecules*, **30**, 3317 (1997).
15. M. L. Glotin and L. Mandelkern, *Colloid Polym. Sci.*, **260**, 182 (1982).
16. R. M. Barrer, *Trans. Faraday Soc.*, **35**, 628 (1939).
17. R. Ash, R. M. Barrer, and D. G. Palmer, *Brit. J. Appl. Phys.*, **16**, 873 (1965).
18. A. M. Shishatskii, Yu. P. Yampolskii, and K. V. Peinemann, *J. Membr. Sci.*, **112**, 275 (1996).
19. F. P. Glatz, R. Mülhaupt, *J. Membr. Sci.*, **90**, 151 (1994).
20. K. Haraya and S. T. Hwang, *J. Membr. Sci.*, **71**, 13 (1992).
21. P. S. Holden, G. A. J. Orchard, and I. M. Ward, *J. Polym. Sci., Polym. Phys. Ed.*, **23**, 709 (1985).
22. A. S. Michaels and R. B. Parker Jr., *J. Polym. Sci.*, **41**, 33 (1959).
23. A. S. Michaels, H. J. Bixler, and H. L. Fein, *J. Appl. Phys.*, **35**, 3165 (1964).
24. H. Fujita, *Fortschr. Hochpolym. Forsch.*, **3**, 1 (1967).
25. S. A. Stern, S. R. Sampat, and S. R. Kulkarni, *J. Polym. Sci., Polym. Phys. Ed.*, **24**, 2149 (1986).
26. R. Chiang and P. J. Flory, *J. Am. Chem. Soc.*, **83**, 2857 (1961).
27. S. A. Stern, S. R. Kulkarni, and H. L. Frisch, *J. Polym. Sci., Polym. Phys. Ed.*, **21**, 467 (1983).
28. W. J. Koros and G. K. Fleming, *J. Membr. Sci.*, **83**, 1 (1993).